

AD-A249 812

PAGE

Form Approved  
OMB No. 0704-0188

2

Public reports  
gathering and  
collection of  
Davis Highway

per response, including the time for reviewing instructions, searching existing data sources, gathering and maintaining the data needed, and completing and reviewing this collection of information. Send comments regarding this burden estimate or any other aspect of this collection of information, including suggestions for reducing this burden, to Washington Headquarters Services, Directorate for Information Operations and Reports, 1215 Jefferson Avenue, Washington, DC 20503.

## 1. AGENCY USE ONLY (Leave blank)

January 13, 1992

## 3. REPORT TYPE AND DATES COVERED

## 4. TITLE AND SUBTITLE

Two-Color Infrared Digital Imaging for Determination of In-Cylinder  
Temperature and Species during Compression and Combustion Periods of  
a DI Diesel Engine

## 5. FUNDING NUMBERS

DAAL03-91-G-0188

## 6. AUTHOR(S)

K. T. Rhce, H. Jiang and Y.I. Jeong

## 7. PERFORMING ORGANIZATION NAME(S) AND ADDRESS(ES)

Rutgers, The State University of New Jersey  
College of Engineering  
Mechanical and Aerospace Engineering  
Piscataway, NJ 08854DTIC  
ELECTE  
APR 30 19928. PERFORMING ORGANIZATION  
REPORT NUMBER

## 9. SPONSORING/MONITORING AGENCY NAME(S) AND ADDRESS(ES)

U. S. Army Research Office  
P. O. Box 12211  
Research Triangle Park, NC 27709-221110. SPONSORING/MONITORING  
AGENCY REPORT NUMBER

ARO 28316.1-EG

## 11. SUPPLEMENTARY NOTES

The view, opinions and/or findings contained in this report are those of the author(s) and should not be construed as an official Department of the Army position, policy, or decision, unless so designated by other documentation.

## 12a. DISTRIBUTION/AVAILABILITY STATEMENT

Approved for public release; distribution unlimited.

## 12b. DISTRIBUTION CODE

## 13. ABSTRACT (Maximum 200 words)

In order to determine the spatial and temporal distributions of temperature and species in a DI diesel engine combustion chamber, development of a new high-speed two-color infrared (IR) digital data system has been conducted. Among the other performed experimental work tasks is the modification of the engine cylinder head in order to accommodate a new optical access assembly. In an attempt to compare the measurement from this work with predictions made by computational method, the KIVA II code has been placed according to our engine specifications. New analytical radiation heat transfer computer programs were developed to evaluate our IR system performance.

Upon completion of the detailed design, the key system components of the IR apparatus have been fabricated and tested, including optical elements and the new electronic packages. At present the mechanical parts composing the assembly are under construction. Our test of the new optical access installed in the engine apparatus exhibits satisfactory results. Preliminary measurements will be obtained soon.

We are in the process of compiling some computational results from the KIVA II operation. According to our results to date, due to many limitations with the code, it appears to be difficult to achieve a realistic evaluation of those results using our measurements from the present experiment. Analysis of our IR system performance using newly developed computer programs suggests that the background radiations (e.g. from the cylinder wall) may not be significant to affect the accuracy of measurements from the gaseous mixtures.

## 14. SUBJECT TERMS

Two-Color, Infrared Spectral, Qualification, Temporal and Spatial Data,  
Distribution of Temperature and Combustion Products, New Electronic Packages15. NUMBER OF PAGES  
21

## 16. PRICE CODE

17. SECURITY CLASSIFICATION  
OF REPORT

UNCLASSIFIED

18. SECURITY CLASSIFICATION  
OF THIS PAGE

UNCLASSIFIED

19. SECURITY CLASSIFICATION  
OF ABSTRACT

UNCLASSIFIED

## 20. LIMITATION OF ABSTRACT

UL

# **Two-Color Infrared Digital Imaging for Determination of In-cylinder Temperature and Species during Compression and Combustion Periods of a DI Diesel Engine**

**K.T. Rhee, H. Jiang and Y.I. Jeong  
Mechanical and Aerospace Engineering Department  
Rutgers, The State University of New Jersey  
New Brunswick, New Jersey 08903  
(908) 932-3651**

## **1. Background**

Among the useful pieces of information to improve the direct injection-type (DI) diesel engine are the spatial and temporal in-cylinder distribution data. They include: (1) the residual gas in the combustion chamber; (2) the temperature and (3) combustion products.

The amount and distribution of residual gas will greatly affect the mixing and ignition of the injected fuel, and consequently the combustion processes that dictate the engine's efficiency and emissions. For example, the low oxygen content and high-temperature in the residual gas will be significant factors affecting the occurrence of ignition.

The determination of timed distributions of in-cylinder temperature and combustion products is highly desirable in improving our knowledge of its physical/chemical processes: This will help find the way to improve the engine with high efficiency and low emissions. In addition, the measurements will enable us to evaluate existing and future engine simulation models.

In spite of the usefulness of such pieces of in-cylinder data, which have long been sought by research individuals, only limited amounts of this information have been obtained in the past. This was mainly due to the absence of versatile tools for implementing the objective. For example, the cylinder species were measured by using the direct sampling method (Brook, 1923; Rhee, et al., 1978); the cylinder gas temperature was measured by using thermocouples (Mure and Rhee, 1989), two-color spectrometry (Wahiduzzaman et al., 1987), and many more. Since those measurements, however, were compiled by using a single probe at a time so that, due to the cyclic variation in the cylinder, the overall in-cylinder picture of the process was difficult to find from such data.

Realizing the limited usefulness of data compiled using those point-measurement methods, we have explored development of a new diagnostic system to obtain "overall pictures," by extending modern advancements in opto-electronic technologies, at Rutgers University during the last several years. The new measurement system was to capture two spectral infrared images at highest framing rates (allowed by the state-of-the-art technology). The raw data was to be processed for determining the spatial and temporal distributions of temperature within the gaseous mixtures in the cylinder, which employs the two-color-ratio IR method.

The design/fabrication of this new high-speed two-color IR digital imaging system was carried out for achieving extensive investigation of not only DI engine combustion processes (under the present sponsorship of the Army Research Office) but also spark-ignition engine combustion (on support from Ford Motor Company).

**92-11547**



**92 4 28 260**

## 2. Objectives

The study was directed to determination of the in-cylinder distributions of temperature and combustion species (water vapor to begin with) from a DI diesel engine using our new high-speed two-color IR imaging system and the results were to be compared with the computational predictions made using KIVA II computer code.

## 3. Results Obtained to Date

In order to implemenent the objectives, several main work tasks were carried out under the present contract (June-December 1991) including:

- (1) Preparation of the engine apparatus;
- (2) Construction of new optical access to accommodate the new IR imaging system;
- (3) Design/fabrication of the high-speed four-color IR imaging system;
- (4) Computational analysis of DI engine combustion using KIVA II; and
- (5) Analysis of system performance and background noise effects on the measurements.

Note that those tasks were performed as continued activities in our laboratory. The award of the present ARO contract led us to perform those tasks in a highly aggressive manner, making our research ability much more potent, otherwise unattainable.

### 3-1. Engine Apparatus

A new single-cylinder high-performance DI engine, designed/built in collaboration with PEI (Beloit, WI) under the U.S. Department of Defense University Research Instrument Program, is being used for the present study. The engine is equipped with engine components from Cummins 903, and electronic-controlled fuel injection system developed by BKM (San Diego, CA). In addition, the apparatus is sufficiently instrumented for performing the present study, e.g. pressure transducer and encorder.

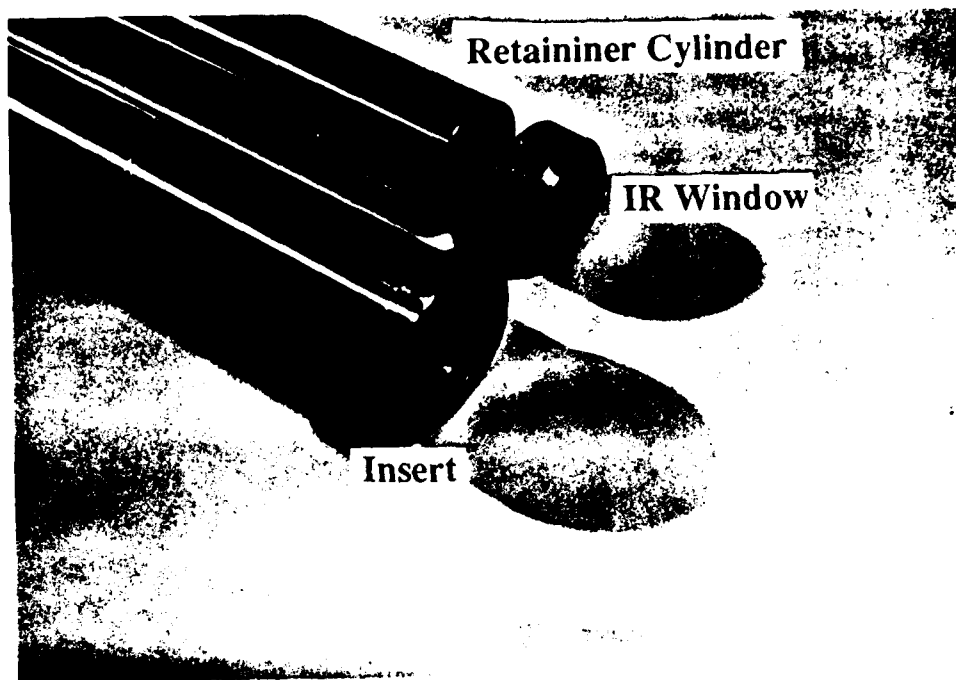
Some modification on the cylinder head was necessary in order to obtain an optical access to the reaction volume. In order to facilitate the modification and to minimize its impacts on the engine combustion processes, it was decided to convert one of two intake valves in the four-valve head. When this conversion was made (in order to accommodate the optical access), a new rocker-arm mechanism was designed/fabricated. The new rocker-arm mechanism on the cylinder head enables us to operate the cylinder head in three-valve mode.

The preliminary tests of the finished rocker-arm assembly exhibit highly satisfactory operations. In order to evaluate the impact of this alteration on the engine combustion, the following steps are being taken: The basic engine performance data were collected from the engine with the original four-valve head during the reporting period. As soon as the fabrication of the cylinder head cover is completed, a similar set of the engine data will be compiled from the new three-valve head equipped engine (with the optical access assembly), which will be compared with those from the original engine setup.

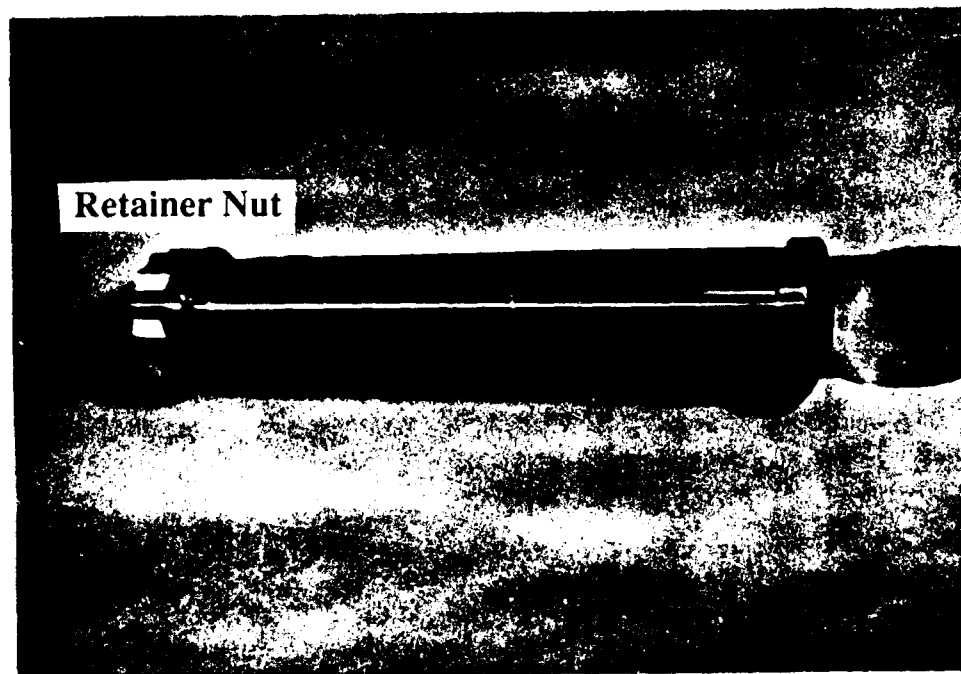
### 3-2. New Design and Fabrication of Optical Access

A new IR window installation method was implemented that employs a wedge-finished Si-window and O-ring seating on an assembly of stainless-steel inserts/mounting components (Figs. 1 and 2).

|  |
|--|
| <input checked="checked" type="checkbox"/> |
| <input type="checkbox"/>                   |
| <input type="checkbox"/>                   |
|  |
|  |
|  |
| Codes                                      |
| Dist and/or Special                        |
| A-1  |



(A) Individual Components of Optical Access (Refer to Fig. 2)



(B) Assembly of Optical Access (Refer to Fig. 2)

**Fig. 1. Optical Access: Individual components and Assembly**  
 (The assembly, upon completion of its bench test,  
 is an integrated part of the cylinder head at present.)

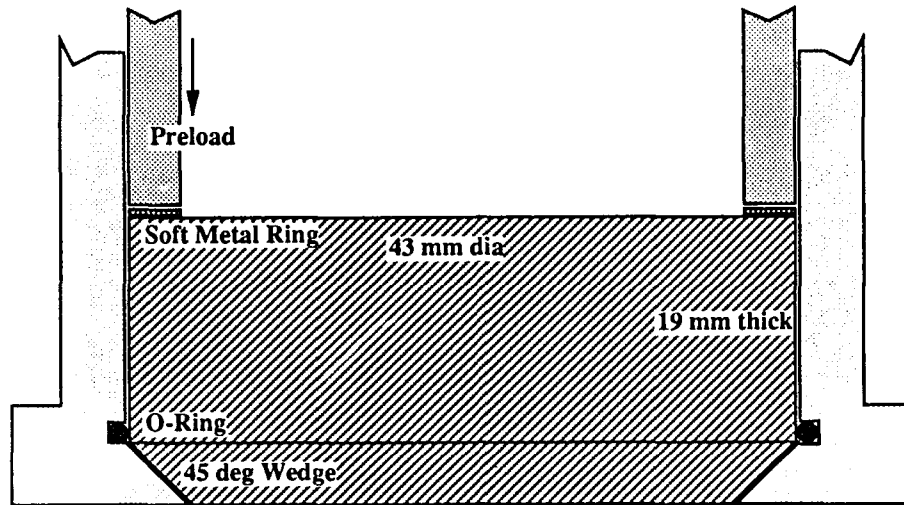


**Fig. 2. IR Window in New Optical Access Assembly**

Among the special considerations taken into account in the design of the new optical access are (1) leakage proof; (2) easy removal/installation of the optical window for cleaning the soot deposit; (3) minimum concentration of preload on the window (in order to avoid its probable damage); (4) facilitation of cooling of the window.

Discussing the new installation method shown in Fig. 2, the O-ring in the stainless-steel insert meets the requirement of leakage-proof. Our room-temperature bench test exhibited no leakage under a pressure of about 2,500 psi. The removal of the window for cleaning was very easy in our assembly, as we evaluated this requirement before we permanently installed (by a cryogenic chill-method) the insert into the cylinder head.

The wedged surface of direct contact was to serve two purposes: spreading the load and increasing the heat transfer. The spreading of the preload over a large area of contact and two directions, i.e., lateral and axial, was to minimize the concentration of load on any single spot of the window. Thanks to the O-ring maintaining a tight sealing, it was found that a little more than a hand tightening (for the preload) was sufficient to avoid the leakage in the above mentioned bench test. The preload on the upper part of the window was made on a copper-ring in order to eliminate again any concentrated sharp load-spot on the window. Note that this area of contact receives the load in one direction only, i.e., axial direction, unlike in the wedged surface on the other side of the window. In addition, the direct contact between the wedged window and the insert surfaces is to increase the heat transfer from the Si-window to the insert (which is cooled by the engine coolant). This consideration was made because of the following reasons: When the Si-window temperature reaches over 250°C, the window becomes a source of radiation emission that will affect the measurements (Zhao, et al. 1991). This potential source of error will be eliminated by cooling the window mentioned above. If additional cooling is required on the window, we have a provision of sending compressed air over the upper surface of the window in order to further remove the heat out of the window.

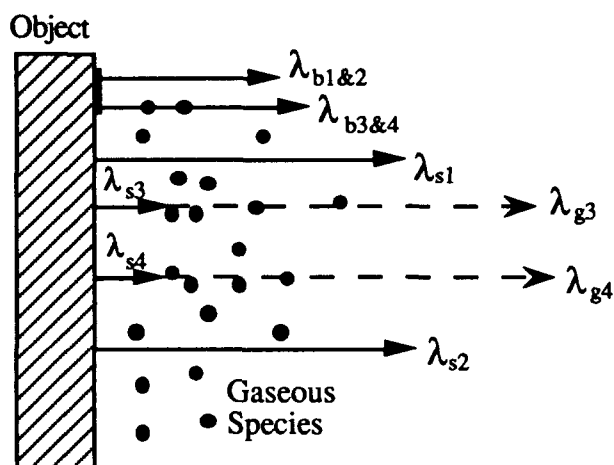


**Fig. 3. Four-Color Spectrometry Concept**

### 3-3. High-Speed Four-Color IR Digital Imaging System

Since the main core of the present study is to complete the development of this new digital imaging system in order to complete accurate and extensive amounts of data from the engine, a greater emphasis is given on the description of the new technique in this report.

When the original proposal was submitted to the ARO, it was to employ two-color IR imaging, as explained above. While the proposal was reviewed by the ARO, we received a new commitment of long-term support from Ford Motor Company who expressed a strong interest in using our new method for the investigation of in-cylinder process in an SI engine. Encouraged by this industrial sponsorship in addition to the present ARO support (for the period June 1991-December 1991), we decided to extend the original two-color ratio method to a four-color spectrometric quantitative imaging method. This extension was made in order to determine the data not only within the gaseous mixtures but also over the combustion chamber surface, as explained below.

#### A. Methodology

In order to explain the methodology of our new device, the radiation from both a solid wall and a gaseous mixture is considered (Fig. 3). Several different radiations emitted from these sources may be listed, having  $\lambda$  represent the central wavelength of each narrow band: They are: (1) surface radiation without being intercepted by the gaseous compound (with wavebands,  $\lambda_{s1}$  and  $\lambda_{s2}$ ); (2) radiation from a blackbody (coating) spot placed on the sample surface (prior to each experiment *for reference*) without being intercepted by gaseous compound ( $\lambda_{b1}$  and  $\lambda_{b2}$ ) and with interception ( $\lambda_{b3}$  and  $\lambda_{b4}$ ); (3) radiation out of an absorbing and emitting gaseous compound resulting from the surface radiation and gas radiation itself ( $\lambda_{g3}$  and  $\lambda_{g4}$ ). Note that subscripts, g, s and b represent the radiation source, gaseous mixture, solid surface and blackbody, respectively.

The idea of the new measurement system is to simultaneously obtain the surface and gas radiations emitted through the line-of-sight in the above four wavebands (i.e.,  $\lambda_1$ ,  $\lambda_2$ ,  $\lambda_3$ , and  $\lambda_4$ ) by using multiple focal plane arrays (FPA) with respective band filters.

It will be further explained (in a new optical arrangement) that the radiation from the solid object (including gaseous compound in front) is split into four separate beams by using our optical train to place four images with an identical geometry but with four individual wavebands.

## B. Temperature over Solid Surface.

Consider the radiations with waveband of  $\lambda_{s1}$  and  $\lambda_{s2}$ , which are nearly transparent to the gaseous compound. One can basically "look (the object wall) through" those wavebands, which is to more accurately determine the surface temperature. This "look-through" approach for the temperature measurement was taken by Bethel and Anderson (1986) by using a single spectrum beam with 3.6-4.0  $\mu\text{m}$  (opposed to two "look-through" wavebands in the present study) in determining the surface temperature variation over the spark-ignition engine combustion chamber. This method had a weakness stemming from the uncertainty of surface emissivity, which is caused by various application factors as explained next.

Such a weakness with this method was anticipated so that when a group of the world's renowned temperature measurement experts gathered together on May 8, 1984 at the National Bureau of Standards (Gaithersburg, MD), they pronounced the various advantages of the *two-color ratio method* for determination of temperature of the solid surface (Richmond and DeWitt, 1984). Note that this method is applicable for the temperature ranging from 150 to 3,000°C. The method was recommended because of its primary application potential on metals, glass, electronics, vacuum chamber, combustion chamber, and various research, where some application factors are involved, e.g. emissivity, target size and movement and contaminated environments (even dirty windows). The most significant advantage of this ratio method is to minimize the effects by those application variables, i.e., by using the ratio method as explained below.

When the two wavebands, having minimum absorption (i.e., "look-through") by the environment gaseous species, are employed, an *advanced* two-color ratio thermometry (for solid surfaces) can be implemented, which compensates for emissivity effects as long as the emissivity ratio,  $\epsilon_1(\lambda_{s1}) / \epsilon_2(\lambda_{s2})$ , is known, where  $\epsilon$  represents emissivity. That is, when there are some changes in the spectral emissivity (due to various causes including temperature change of the surface), such effects are cancelled if the ratio is used: Suppose an output,  $S$  is measured (e.g., in volts by using a detector) at two different wavelengths,

$$S_1 = K_1 \epsilon_{\lambda 1}(\lambda_{s1}) E_{\lambda b}(\lambda_{s1}, T) \text{ and}$$

$$S_2 = K_2 \epsilon_{\lambda 2}(\lambda_{s2}) E_{\lambda b}(\lambda_{s2}, T).$$

where  $K_1$  and  $K_2$ , or ratio, may be determined by calibration in terms of a blackbody or even gray body, and  $E$  represents emission power. From the ratio  $R(T)$  of the measured signals, and by substituting from Wien's law for  $E_{\lambda b}(\lambda, T)$ , we obtain

$$\begin{aligned} R(T) &= S_1(T) / S_2(T) \\ &= (K_1 / K_2) (\epsilon_{\lambda 1} / \epsilon_{\lambda 2}) \text{Exp} \{-C (1/\lambda_{s1} - 1/\lambda_{s2}) / T\} \dots\dots\dots(1) \end{aligned}$$

which can be solved for the temperature, since all other quantities are known.

Because of its great usefulness, this method has widely been realized in recent years, particularly by the steel industry in development of high-strength steels. Note that their measurement devices are limited to the single-point measurement, opposed to the area measurement to be achieved by the proposed study. Our present choice of two wavebands for surface temperature measurement are 2.055-2.155 and 3.763-3.938  $\mu\text{m}$ , which are transparent to most species in even the hydrocarbon-fuel combustion environment.

### C. Temperature of the Gaseous Flow around the Object.

Although the stagnation temperature of a gaseous compound around (and bouncing off) the object surface may be predicted, its measurement and the flow field can be determined using two gaseous radiations with  $\lambda_{g3}$  and  $\lambda_{g4}$ . Note that others employed it for temperature measurement of in-cylinder gaseous mixture: Matsui, et al.(1980) employed wavelengths of 2.3 and 4.0  $\mu\text{m}$  and Wahiduzzaman, et al. (1987) used those of 1.3 and 2.3  $\mu\text{m}$ .

In spite of its similar advantages to those for surface temperature measurement mentioned above, one of the weaknesses of this method may be the unavailability of the surface radiation (i.e., those with  $\lambda_{s3}$  and  $\lambda_{s4}$  in Fig. 3) simply because the temperature and emissivity of the surface were not available in their in-cylinder measurements. This problem, however, will be eliminated in our four-color method: A coating (at selected spots) with blackbody emissivity (or any thin coating with known emissivity) is placed on the object prior to the experiment. This is to find the spectral surface emissivity by comparing emissions with  $\lambda_{b1}$  and  $\lambda_{b2}$  to those with  $\lambda_{s1}$  and  $\lambda_{s2}$ , respectively. Since the wavelengths are not very much apart from each other, it is reasonable to calculate spectral emissivities at  $\lambda_3$  and  $\lambda_4$  by interpolation. Note that this prediction may be checked by comparing radiations with  $\lambda_{b3}$  and  $\lambda_{b4}$  with those  $\lambda_{s3}$  and  $\lambda_{s4}$ . When the emissivities at  $\lambda_3$  and  $\lambda_4$  are determined, it is straightforward to find surface radiation at  $\lambda_{s3}$  and  $\lambda_{s4}$  in order to have an improved computation of gas temperature using the conventional two-color method. (Our present choice of two wavebands (water vapor bands) for determining temperature distribution in the flow are 2.445-2.495 and 5.115-5.385  $\mu\text{m}$ .) The results from this method, i.e.,  $\epsilon_{s1}$  and  $\epsilon_{s2}$ , may also be introduced into Eq. (1) for the surface temperature measurement. Once the temperature of the gaseous compound is known, its concentration distribution can also be calculated by using our user-friendly software.

**Remarks.** Our new four-color method is to simultaneously capture four images in respective IR spectral bands at high framing rates with ultra short exposure periods: This will enable us to determine the distribution of temperature over *the object* using a pair of images and to find the similar distribution in *the flow* by using the remaining pair of images.

**Scope of Applications.** The new system will enable us to investigate many demanding problems. The uniqueness of the methodology includes:

- (1) the imaging is made at very high framing rates;
- (2) the imaging is made with very short exposure periods; and
- (3) multispectra images are obtained to quantify various chemical/thermal characteristics;



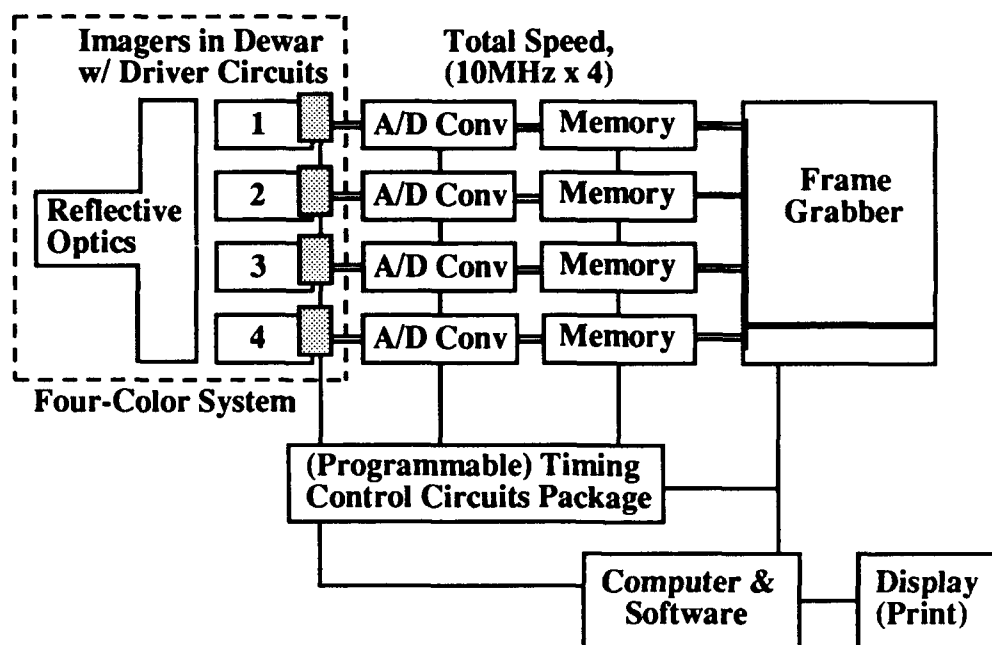


**Fig. 4. Parallel-Process High-Speed Digital Imaging System**

#### **D. Description of New System Apparatus**

The system is to achieve a parallel processing of the data acquisition in order to obtain in-depth information as to the reaction in the gaseous mixture as well as the thermal characteristics of the cylinder wall surface. Figure 4 schematically shows the system arrangement. The reflective optical apparatus places four spectral images on respective imagers housed in each cryogenic dewar. Upon receipt of photons over the sensing area of the imager, the individual pixels will produce negative charges according to the number of photons they absorb. Once the exposure period is over, i.e., at the end of integration of photon receipt, the charges will have to be read out in an orderly manner through the charge-coupled devices (CCD) scheme.

In order to achieve this, the timing circuits will generate four-phase master timing signals which are sent to the differential driver circuits. The driver circuits will generate about fifteen (15) distinctive signals (using the received master timing signals) and their strength, i.e., powers are sufficiently amplified to drive the respective imager and read out the charges from individual pixels.

The master signals are also sent to A/D boards, which determines the sampling time of the video signal for A/D conversion. In addition, the same signals are provided to the memory boards so that the digitized data are stored in a controlled fashion. Once the measurement is completed, say to compile about 250 frames of image in each memory, the data is retrieved by using our frame grabber to send them to our larger data storage which is incorporated with the desk-top computer.

**Optical Arrangement.** The four spectral images mentioned above will be obtained using the new optical system shown in a drawing (Fig. 5) in reduced scale, 25%. The radiation from the object is captured by the primary mirror which is spectrally split into two parts, i.e., reflection of the short-wavelength radiation and transmission of the long-

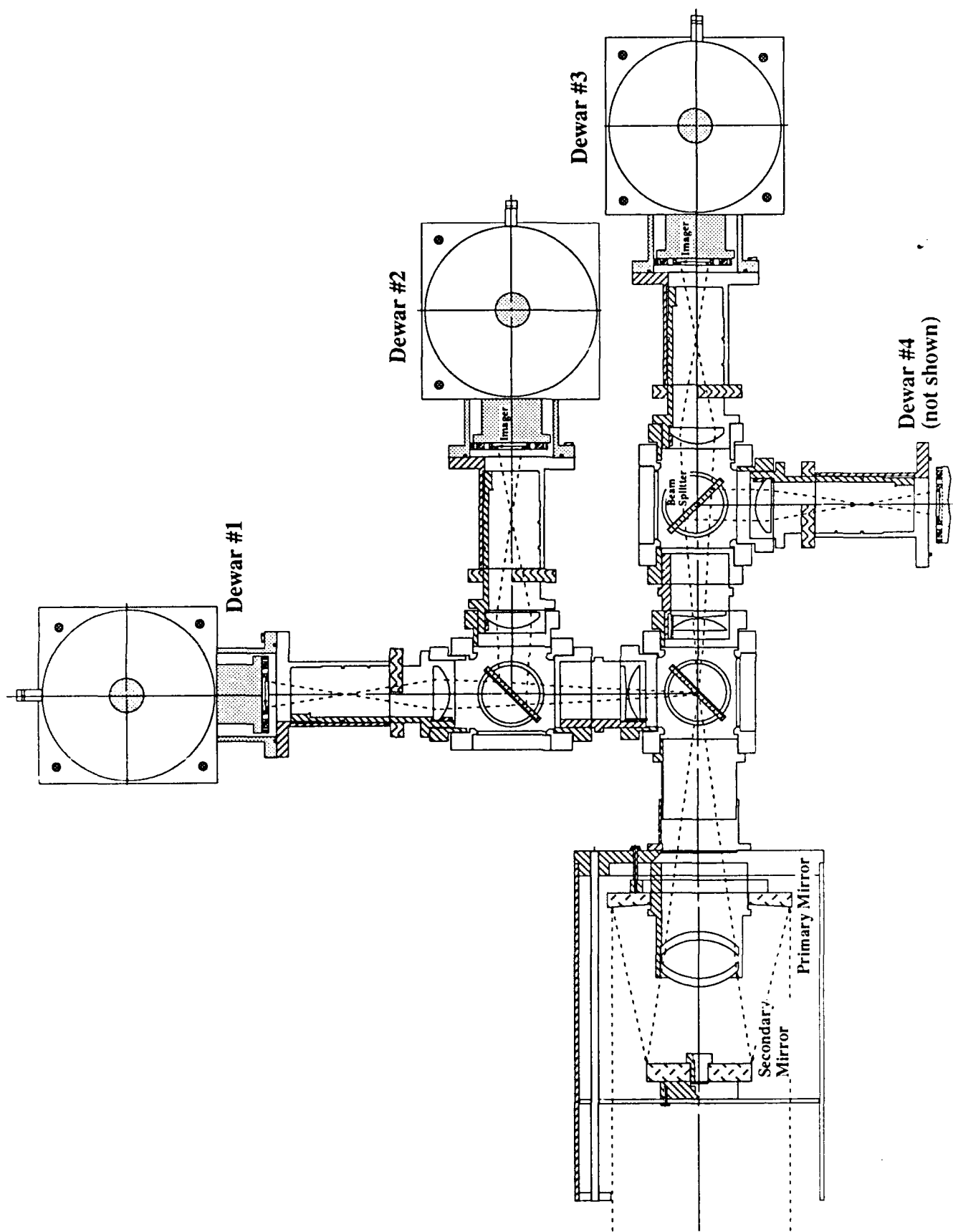


Fig. 5. Assembly Drawing of Four-Color Imaging System with Reflective Optics Arrangement

wavelength radiation. These beams will be followed by an additional splitting respectively, which will result in placement of four respective spectral images on corresponding imagers in nitrogen-cooled dewars.

The optical components of the system have been fully fabricated by Republic Lens (Englewood, NJ). What is preventing us from making further progress is the delayed fabrication of the mechanical components that place the optical components. As one can find from Fig. 5, there are more than fifty-six (56) mechanical components required for precision machining for completing the assembly. We expect to complete their fabrication within about one month from this reporting time. As soon as they become available to us, the assembling and testing of the apparatus will be made.

**Timing Boards.** As briefly mentioned above, we will need four separate electronic driving circuit packages to read out the signals from the imagers, which receive the identical sets of timing signals from the timing board using one master (crystal) clock. It is worthy to mention that unique design of this timing circuit enabled us to obtain some extraordinary imaging performance using off-the-shelf item imagers, which is far more than what the original imager developer achieved. In addition, our timing circuit is being incorporated with programmable logic gate arrays. This allows us to find the most desirable imager driving scheme (by basically trial and error in order to extend its performance up to the limit). Note that this search of optimum electronic package is not easy to attain without the versatility and flexibility in the circuitry design.

**A/D Converter Boards.** Four A/D converter circuit packages and memory boards are assigned in order to process the analog signal (i.e., video output from the imagers). The digital data stored in our memory system newly designed/fabricated in our laboratory will be retrieved by using the conventional frame grabber. Note that the amount of data to be stored in our memory can be expanded but the present package will hold as many as 256 frames (64x64 in 12-bit in each frame) per memory board in each measurement.

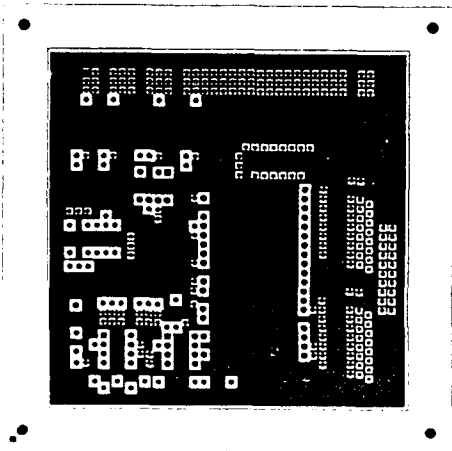
Upon the successful construction of the prototype board (by hand-wiring), we constructed the package in printed boards, which eliminated the electronic noises modulated into the package (Fig. 6).

### **3-4. Computational Analysis of DI Combustion Using KIVA II Code**

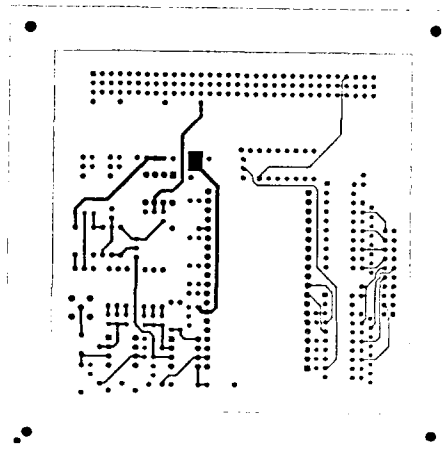
In an attempt to compare our experimental data to be obtained using the present system with the computational prediction made using the KIVA II code, we have struggled to learn its installation/operation and retrieval/plotting of the results for some time. We are still in the middle of many questions as to the use of the code and interpretation of the results (but we are beginning to compile the computational results).

For example, even a small change in the grid generation from the ones shown in Fig. 7-(A) produced a significant impact on the pressure-time data, which was often greater than effects of important combustion parameters. Since there are many initial engine conditions to be assumed in order to run the code, including assumption of the gas motions after the intake valve closing, the results from this work may not be realistically compared with those from the experiment. Some typical examples from this computational work are included in Fig. 7-(B) without further elaboration.

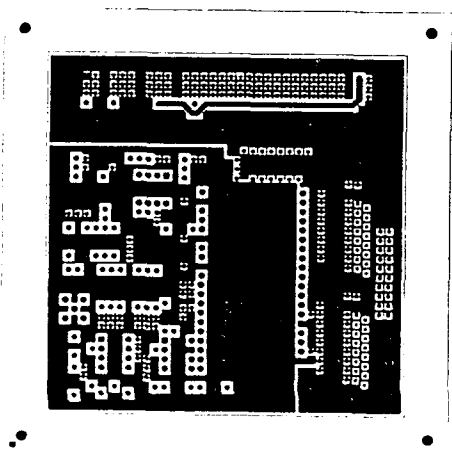
We will continue these computational activities in order to achieve "reconciliation" of the code operation with the basic engine measurement such as pressure-time data prior to attempting any in-cylinder data comparison with the predictions.



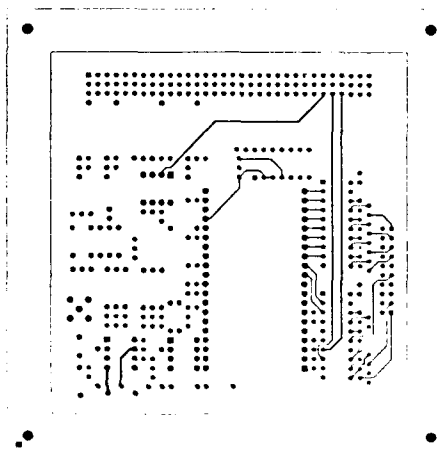
Layer -1



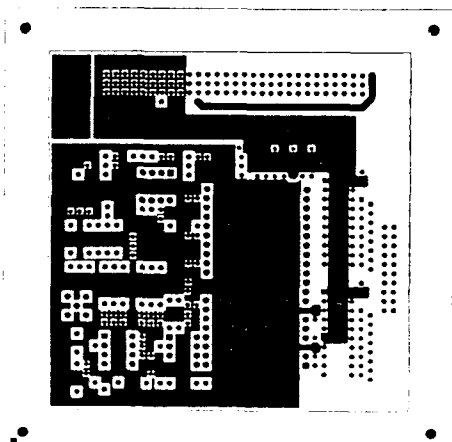
Layer-2



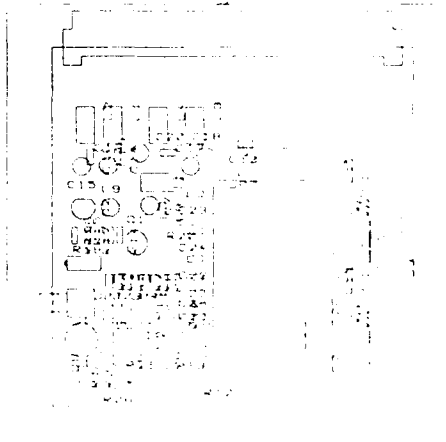
Layer -3



Layer-4



Layer -5



Layout

**Fig. 6 New A/D Converter Circuit Module Board:  
Five-Layer Art Work & Layoput of the Board.  
(45% of the Actual Size)**

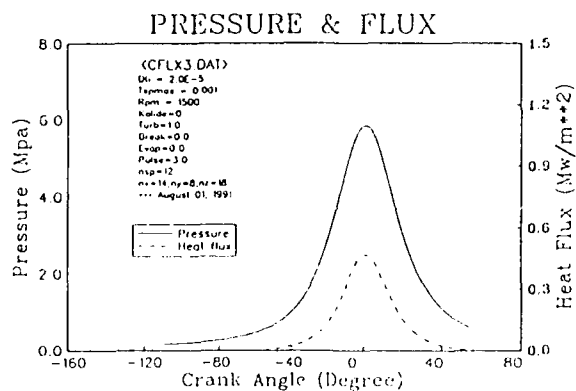
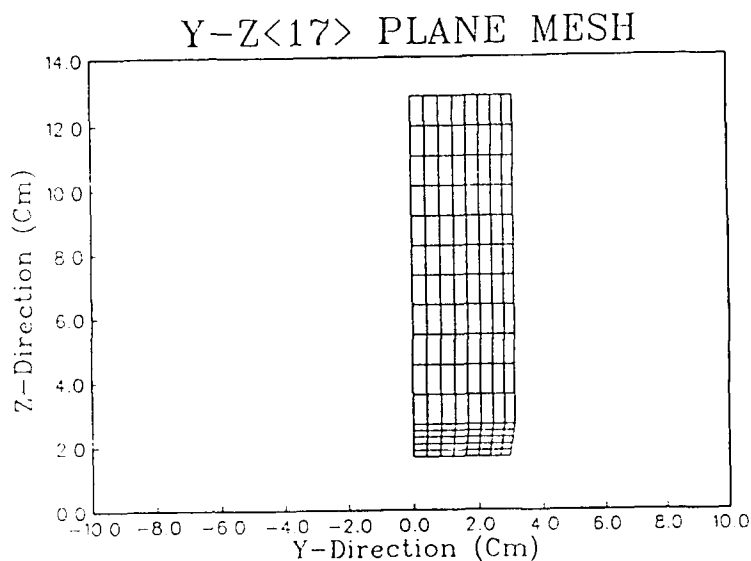
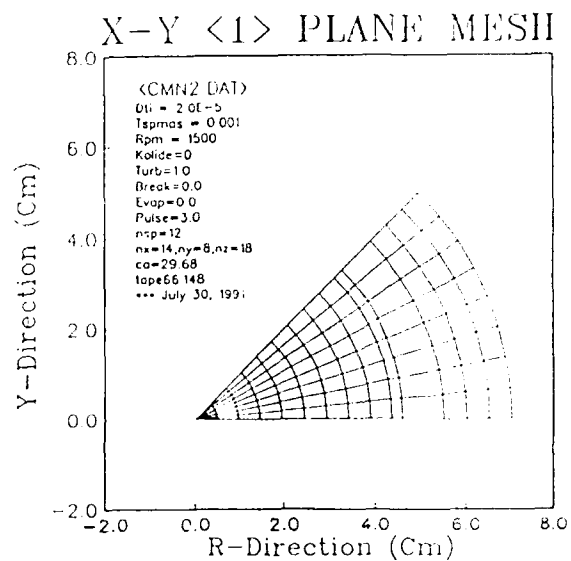
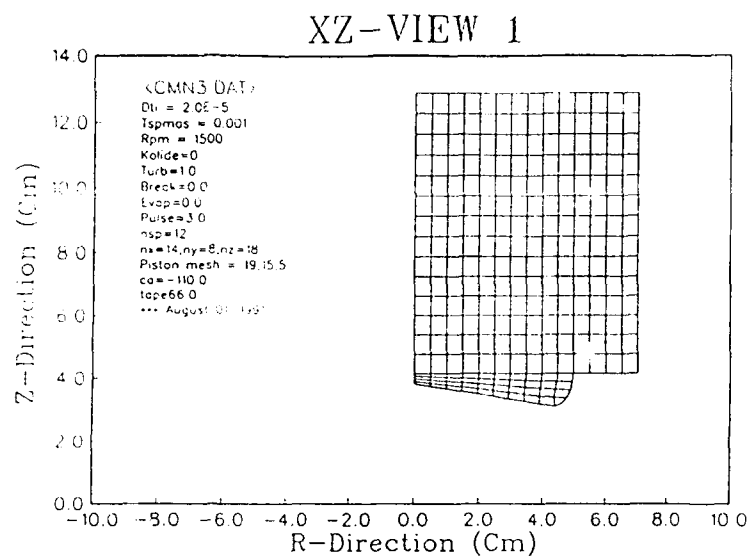


**Fig. 7-(A). Grid Generation used for Producing Pressure-time and Heat Release Prediction**

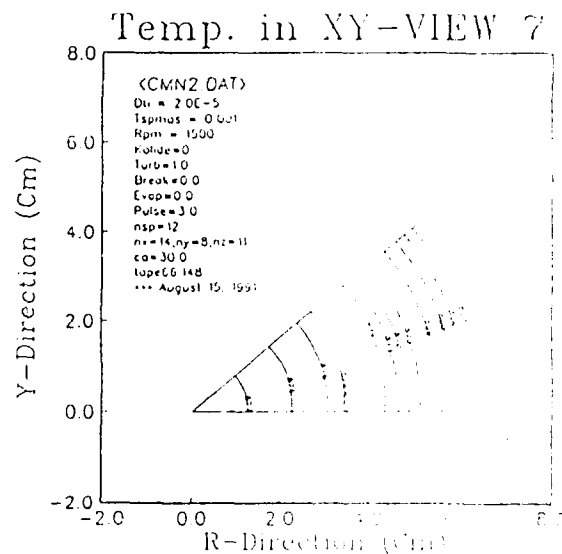
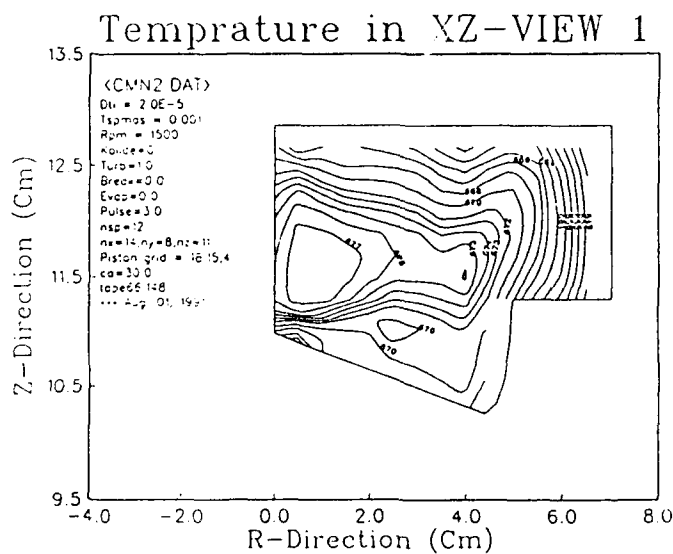
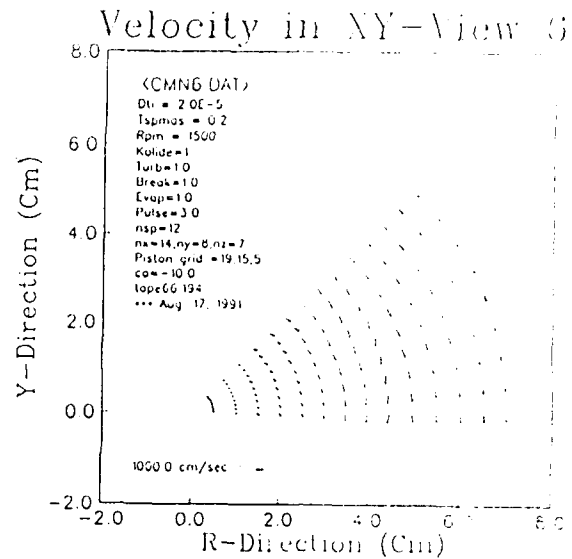
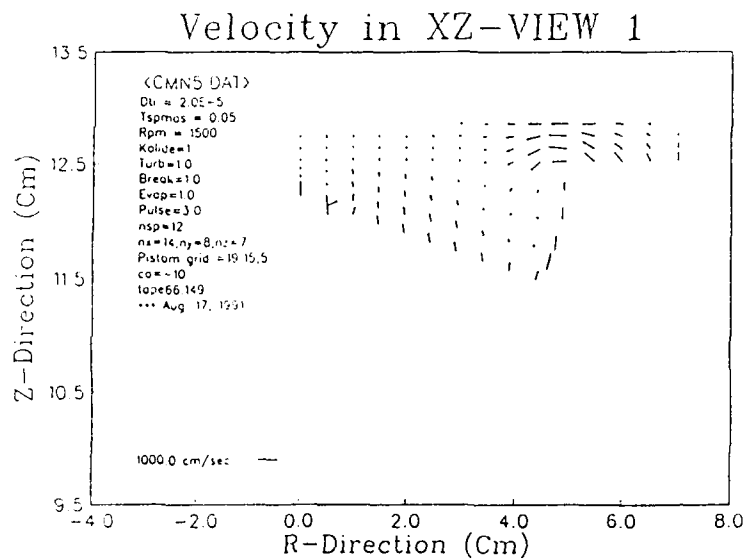


**Fig. 7-(B). In-Cylinder Distributions of Gas Motions and Temperature Predicted using KIVA II of our DI Engine**

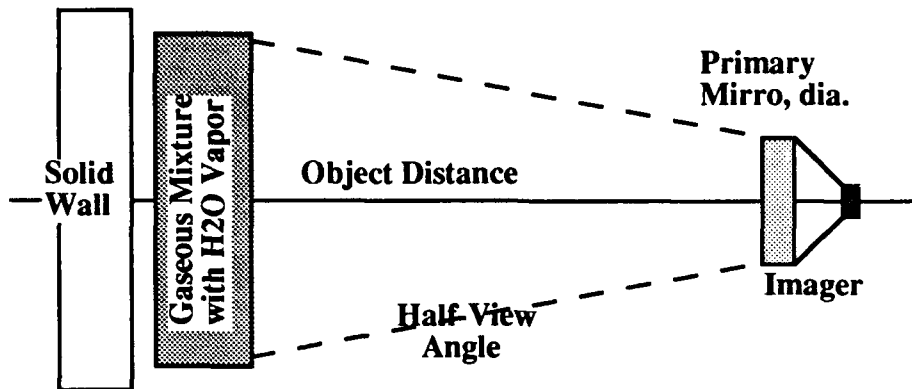


**Fig. 8. Schematics of Radiation Emission from Wall and Residual Gas Containing Water Vapor at Some Measurement Conditions**

### 3-5. Analysis of Performance of Our New IR Imaging System

The reviewers of our proposal expressed some concern as to the possibility of "outshining" the emission from the target gaseous mixtures by the radiation from the engine cylinder surface. (It was indicated by the program director, Dr. D. Mann, to evaluate as a part of the activities in the present study.) In order to clarify this important issue, we have taken two approaches while the actual imaging system is being fabricated and the engine cylinder is modified for accommodating the new diagnostic system. They are: (1) computational analysis and (2) bench test.

We have developed three new menu-guided computer programs in order to calculate the output from our pixels in the imager. Since it is to compare the computational results with measurements from our imaging apparatus using a new bench setup, the computer programs were constructed with inclusion of not only radiation source characteristics but other key system information. They are the geometric configuration, the optical train design, IR imager responsivity to the radiation in individual spectral bands, and others. Consequently, the computed result is produced in terms of voltage output from the individual pixels in our imaging system according to specified measurement conditions (See Fig. 8). The input information required in the computation by using the programs are:

- . Pixel size;
- . Temperature range of the wall or gaseous mixture;
- . Size of temperature step for computation;
- . Wave band range of radiation (filter band);
- . Pressure;
- . Concentration of water vapor or CO<sub>2</sub>;
- . Size of concentration step for computation;
- . Length (physical) of the gaseous mixture volume;
- . Object distance;
- . Half-view angle of optical path
- . Lens diameter; and
- . Exposure period of the imager.

The above list is included here in order to indicate what variables are considered in the computation programs and the discussion on the models is made only in brief. The first to mention in the list is the need for the pixel size data input: Although the responsivity data (charge generated/radiation energy received by pixel) of PtSi pixel reported in literature was included in the model (Kosonocky, 1990), it is required in the computation because the size of the pixel proportionately dictates the amount of negative charge built up in the different imagers. (Note that we employ two types at present 64x128 and 320x244 imagers.) Since the response range of our imager is 1.1-5.5  $\mu\text{m}$ , the gas radiation data (Ludwig et al., 1973) included in our models were limited to the corresponding range. Some assumptions were employed in the programs: the solid surface is a black body; the gaseous mixture is uniform and homogeneous, and the multiple line and single line group models with Curtis-Gordon approximation (Ludwig et al, 1973) is applicable; and no loss of radiation energy (due to absorption/reflection by lens, filter and others) is considered. The actual measurements will be, therefore, lower than the computed output (in volt) from the pixel by factor of the spectral emissivity of the wall and transmittance of the optical train, which is taken into account in the data interpretation.

Some of the results from the analysis are explained below. The pixel output from the residual gas mixture containing water vapor at about ten atmospheric pressure (during the compression period) was calculated as shown in Fig. 9-(A). The output from the pixel ranges from 0.1 to 2.7 volts, which is a very high signal strength.

The pixel output from the solid wall (without the gaseous mixture in front) was similarly calculated as indicated in Fig. 9-(B). The signal strength ranges from 0.1 to 0.7 volts. This suggests that the "outshining" by the surface radiation is negligible as long as the cylinder wall temperature is lower than 550K. It is noted that this comparison is made in order to investigate the most adverse measurement condition: When the gas temperature is higher than considered here, as expected during the injection or combustion period, the emission from water vapor will far overshadow that from the background radiation.

The computational results mentioned above offer highly favorable predictions as to the background radiation effects on the target measurement. In order to systematically evaluate these findings, an existing bench apparatus is being modified at present (Fig. 10). This bench apparatus will enable us to simulate the actual measurement conditions specified in Figs. 9-(A) and -(B). Note that the physical size of the optical path is rather long in the device. This measure was employed in order to go around the need for the elevated gas pressure in the chamber, which is difficult to achieve at a reasonable cost.

The actual experiment mentioned above has not been carried out due to the delay in the construction of mechanical components required for the assembly of the optical train. As soon as the testing of the system assembly is completed, this evaluation work will be performed in order to confirm the prediction made using our computer models.

#### 4. Conclusion

Several main work tasks were carried out during the period of six months under the present ARO sponsorship, which include (1) preparation of the engine apparatus; (2) construction of new optical access to accommodate the new IR imaging system; (3) design/fabrication of the high-speed four-color IR imaging system; (4) computational analysis of DI engine combustion using KIVA II; and (5) analysis of system performance and background effects on the measurements. Several findings worthy of note are listed below:



### Measurement Condition

|   |                     |
|---|---------------------|
| Imager (Pixel Size).....                              | 320x244             |
| Temperature range of the wall or gaseous mixture..... | 473-673 (K)         |
| Size of temperature step for computation.....         | 5.0 (K)             |
| Wave band range of radiation (filter band).....       | 2.45-2.49 ( $\mu$ ) |
| Pressure.....   | 10 (atm)            |
| Concentration of H <sub>2</sub> O.....                | 0.5-10 (%)          |
| Size of concentration step for computation.....       | 0.5                 |
| Length (physical) of the gaseous mixture volume.....  | 5.0 (cm)            |
| Emissivity of the surface.....                        | NA                  |
| Object distance.....                                  | 40 (cm)             |
| Half-view angle of optical path.....                  | 5.0 (deg)           |
| Lens diameter.....                                    | 150 (mm)            |
| Exposure period of the imager.....                    | 0.5 (msec)          |

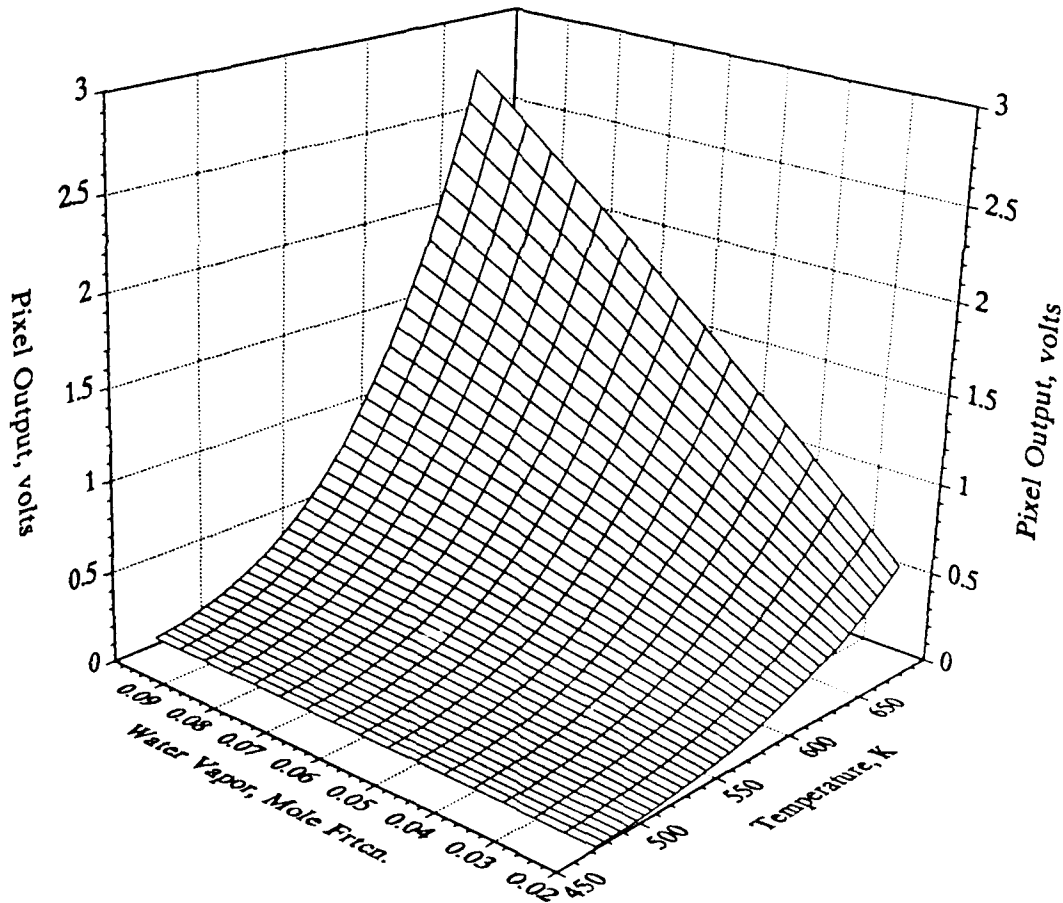


**Fig. 9-(A). Pixel Output vs. Temperature of Object:  
Residual Gas Containing Water Vapor at 473-673  
during the Early Compression Period.**

### Measurement Condition

|   |                     |
|---|---------------------|
| Imager (Pixel Size).....                              | 320x244             |
| Temperature range of the wall or gaseous mixture..... | 373-573 (K)         |
| Size of temperature step for computation.....         | 2.0 (K)             |
| Wave band range of radiation (filter band).....       | 2.45-2.49 ( $\mu$ ) |
| Pressure.....   | NA                  |
| Concentration of water vapor or CO <sub>2</sub> ..... | NA                  |
| Size of concentration step for computation.....       | NA                  |
| Length (physical) of the gaseous mixture volume.....  | NA                  |
| Emissivity of the surface.....                        | 0.85                |
| Object distance.....                                  | 45 (cm)             |
| Half-view angle of optical path.....                  | 5.0 (deg)           |
| Lens diameter.....                                    | 150 (mm)            |
| Exposure period of the imager.....                    | 0.2 (msec)          |

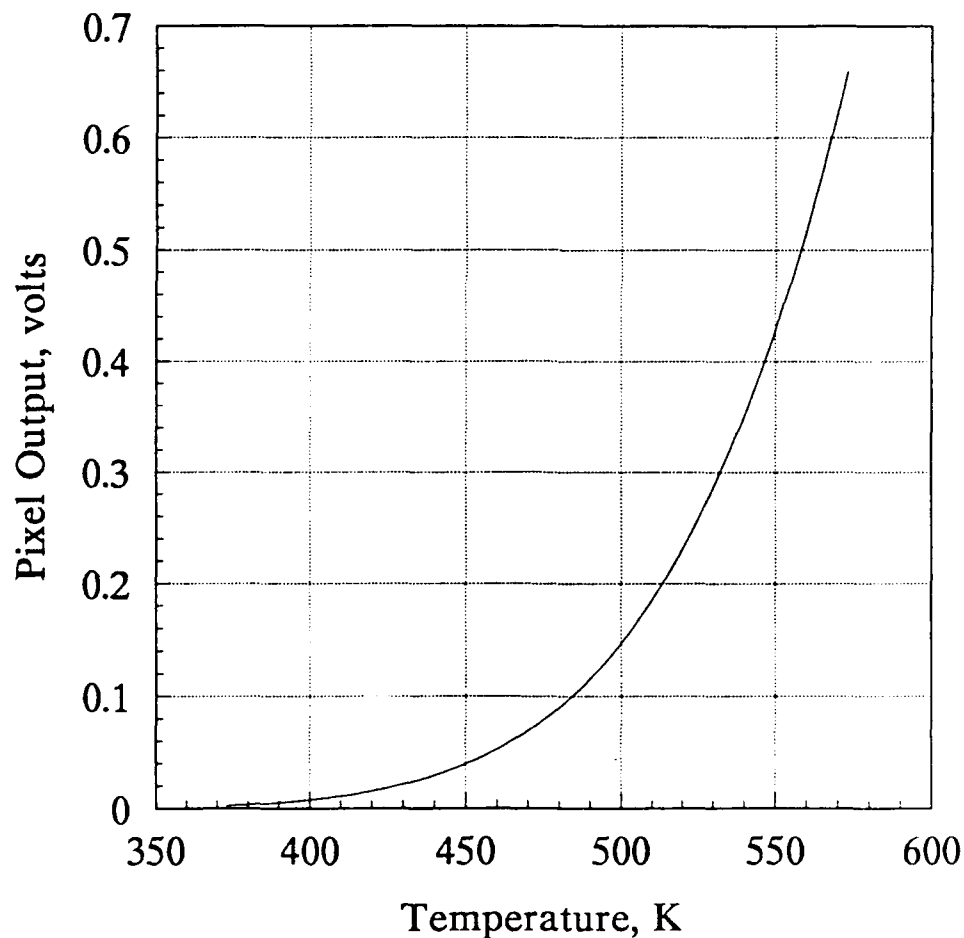
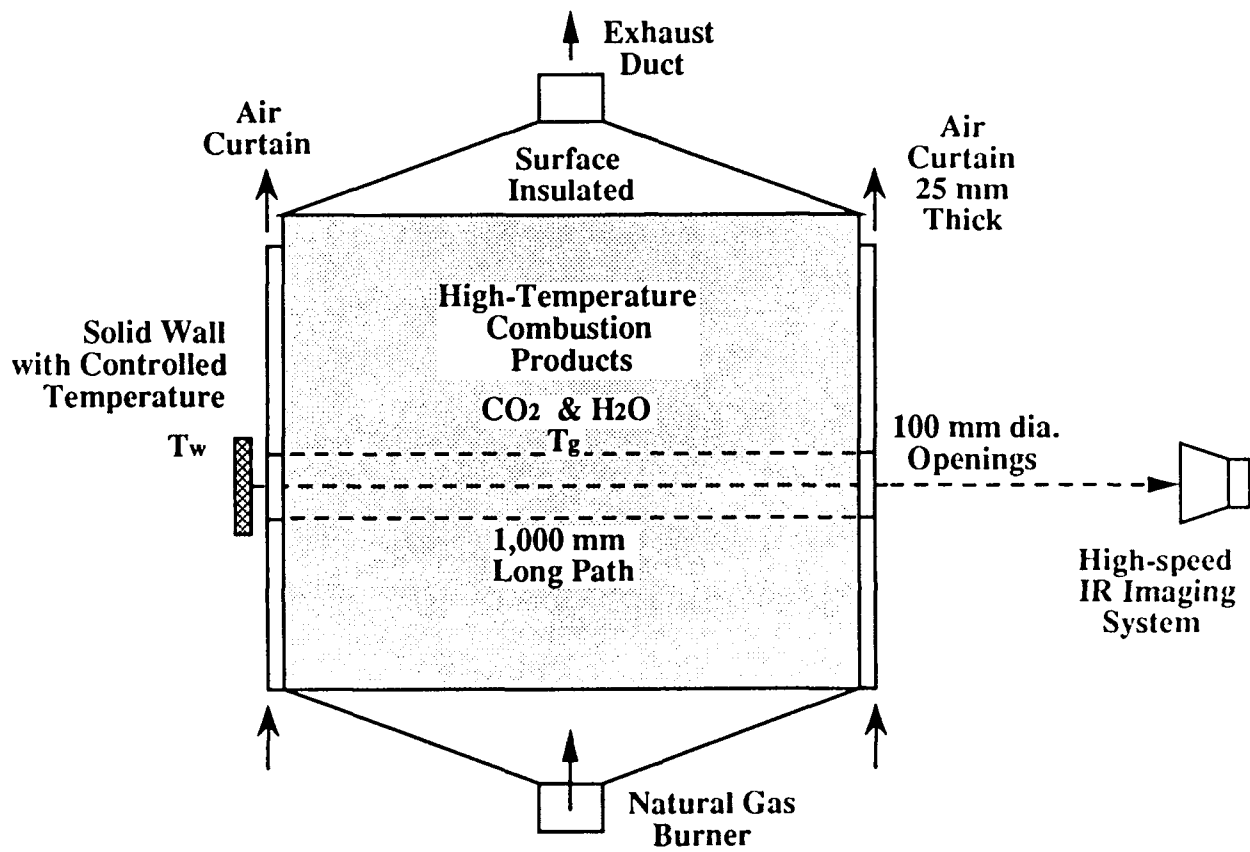


Fig. 9-(B). Pixel Output vs. Temperature of Object:  
Solid Wall at 373-573K.



**Fig. 10. A Bench Set-up for Examining Radiation Emission from Controlled Combustion Products and Background Wall**

. The initial test of the modified engine rocker-arm assembly exhibited satisfactory operations, which will be further tested as soon as the cylinder head cover construction is completed.

. The new method of producing the optical access was introduced that maximizes the flexibility of experiment and minimizes potential background (thermal) noises.

. The greater portion of the high-speed spectral IR imaging system has been constructed to date, including the entire optical elements and new electronic circuit packages. As soon as the mechanical components are completed, the system assembly will be tested.

. We are in the process of producing some preliminary results from the computational analysis of the DI engine combustion by using the KIVA II code. At present, it seems to be somewhat limitedly optimistic in comparing the results from this work with the experimental results, however.

. According to our performance analysis of the present IR imaging system using newly developed computer programs, the background noise (i.e., radiations from the cylinder wall in the opposite side of the gaseous mixture) is very likely to be negligible. This will, however, be further evacuate using a new bench apparatus.

## **5. Future Activities.**

We expect to complete the mechanical components which position the optical elements in the system assembly, within about a month from this reporting time. The optics specialist in charge of assembling and testing of the unit will complete the apparatus.

We will continue to refine the electronics package which are proven to be functional, yet need further adjustment.

The engine set up appears to be ready but the final testing remains to be done. The optical access built in the cylinder head will also be tested under the firing conditions.

The computational analysis of the DI engine will be further conducted in order to find some meaningful results, which is to explore if the code can be verified by using the measurements from the present experiment.

The background noise which might be a factor affecting our measurement from the gaseous mixture will be evaluated using the bench apparatus that has been already fabricated.

Once the testing of individual units is complete, we will obtain some preliminary results to find if there are further needs for adjustment/improvement in each unit and the total system. Upon completing the evaluation of results in this stage, a parametric study of the DI engine processes will be performed in order to increase our understanding of the in-cylinder events of the engine.

## 6. References

- Bethel, S. and Anderson, C.L., "An Infrared Technique for Measuring Cycle-resolved Transient Comb. Chamber Surface Temp. in Fired Engine, SAE Paper-860240, 1986.
- Brooks, D. B., "Chemistry of Internal Combustion Engines," M.S. Thesis, Ohio State University, May 1922.
- Kosonocky, W.F., "Review of Schottky-Barrier Imager Technology," SPIE Proceedings, Vol. 1308, Infrared Detectors and Focal Plane Arrays, April 1990.
- Ludwig, C.B., Malkmus, W., Reardon, J.E., and Thomson, J.A.L., Handbook of Infrared Radiation from Combustion Gases, NASA SP-3080, 1973
- Matsui, Y., Kamimoto, T., and Matusoka, S., "A Study on the Application of the Two-color Method to Measurement. of Flame-- in Diesel Engine," SAE Paper-800970, 1980.
- Mure, C. and Rhee, K.T., "Instantaneous Heat Transfer over the Piston of a Motored Direct Injection-type Diesel Engine," SAE Paper-890469, 1989.
- Rhee, K.T., Uyehare, O.A. and Myers, P.S., "Time- and Space-Resolved Species Determination in Diesel Combustion using Continuous Sampling," SAE Paper-780226, 1978.
- Richmond J.C. and DeWitt, D.P., Application of Radiation Thermometry, ASTM Special Tech. Publication 895, ASTM, Philadelphia, Pa., 1984.
- Wahiduzzaman, S., Morel, T., Timer, J. and DeWitt, D.P., "Experimental and Analytical Study of Heat Radiation in a Diesel Engine," SAE Paper-870511, 1987.
- Zhao, H., Collings, N. and Ma, T., "The Cylinder Head Temperature Measurement by Thermal Imaging Technique," SAE Paper-912404, 1991